Arif Zamir Khan

› Study of the correlation of J/psi production with event multiplicity in pp collisions using the PYTHIA 8 event generator

2025

Study of the correlation of J/psi production with event multiplicity in pp collisions using the PYTHIA 8 event generator

Bachelor thesis
submitted to the

Universität Münster
Institut für Kernphysik

by
Arif Zamir Khan

March 2025

First examiner:	Prof. Dr. Anton Andronic
Second examiner:	Apl. Prof. Dr. Christian Klein-Bösing
Day of submission:	Friday 28th March, 2025

Abstract

In this thesis the self normalized mid-rapidity J/ψ yield as a function of self normalized charged particle multiplicity was studied for simulations involving pp collisions at a center of mass energy of $\sqrt{s} = 13\,\mathrm{TeV}$ using the PYTHIA 8 event generator. Different charged particle rapidites and regions were investigated. Previous investigations attributed the stronger than linear increase to autocorrelation effects [Web19]. Autocorrelation effects happen due to physical processes that cause the J/ψ yield to influence the charged particle multiplicity, meaning that these two quantities are not independent. These effects correspond to a stronger than linear increase combined with a high dependence on the transverse momentum p_T. In this thesis different rapidity ranges of the charged particles were studied, and it could be confirmed that autocorrelation effects explain the stronger than linear increase. It could also be confirmed that charged particles in the transverse region with respect to the J/ψ flight direction minimize autocorrelation effects. The studied ranges for the charged particle rapidity η were $|\eta| < 1$, $1 < \eta < 2$, $2 < \eta < 3.5$ and $3.5 < \eta < 5$. Out of these rapidities $|\eta| < 1$ exhibits the strongest autocorrelation effects, $1 < \eta < 2$ and $2 < \eta < 3.5$ exhibit some weak autocorrelation effects and $3.5 < \eta < 5$ shows very weak to no autocorrelation effects.

Declaration of Academic Integrity

I hereby confirm that this thesis, entitled "Study of the correlation of J/psi production with event multiplicity in pp collisions using the PYTHIA 8 event generator" is solely my own work and that I have used no sources or aids other than the ones stated. All passages in my thesis for which other sources, including electronic media, have been used, be it direct quotes or content references, have been acknowledged as such and the sources cited. I am aware that plagiarism is considered an act of deception which can result in sanction in accordance with the examination regulations.

_____

(date, signature of student)

I consent to having my thesis cross-checked with other texts to identify possible similarities and to having it stored in a database for this purpose.

I confirm that I have not submitted the following thesis in part or whole as an examination paper before.

_____

(date, signature of student)

Contents

1 Introduction

Particle collisions are an important physical process, of which the study can give a lot of insight about how the universe operates at a fundamental level. They involve physical phenomena which may explain the early stages of the universe, and the most basic particles that make it up [CER]. Some of these particles are quarks, which make up other particles like e.g. protons, neutrons, or J/ψ mesons, which will be the subject of interest of this thesis.

In previous experimental measurements it has been found, that there is a stronger than linear increase of mid-rapidity J/ψ yield as a function of self normalized charged particle multiplicity. This has been studied in the ALICE experiment at the LHC [Abe12]. Simulations can be a powerful tool to study this behaviour. That is why the PYTHIA 8 event generator is used in this thesis. In order to explain this behaviour, there are theoretical models that have been put forward [FP12]. However, in a previous article, also involving the PYTHIA 8 event generator, this behaviour was attributed to autocorrelation effects. That means, it was considered that the charged particle multiplicity and J/ψ yield are not independent quantities, but that the J/ψ yield influences the charged particle multiplicity. From investigating that it was concluded that this fact is responsible for the stronger than linear increase [Web19].

In this thesis the self normalized mid-rapidity J/ψ yield is studied as a function of charged particle multiplicity for different rapidity ranges, and it is investigated whether these autocorrelation effects indeed explain stronger than linear behaviour for other rapidity ranges and if analogous behaviour can be found. For this different production processes and transverse momentum intervals are also analyzed. We go beyond previous studies, which explain experimental data, and look at rapidity

ranges that have not been studied experimentally in the ALICE experiment, which is an additional benefit of simulations.

2 Theoretical background

2.1 The standard model

The standard model consists of different elementary particles and is used to describe all known fundamental forces with the exception of gravity, as well as all elementary particles that make up matter.

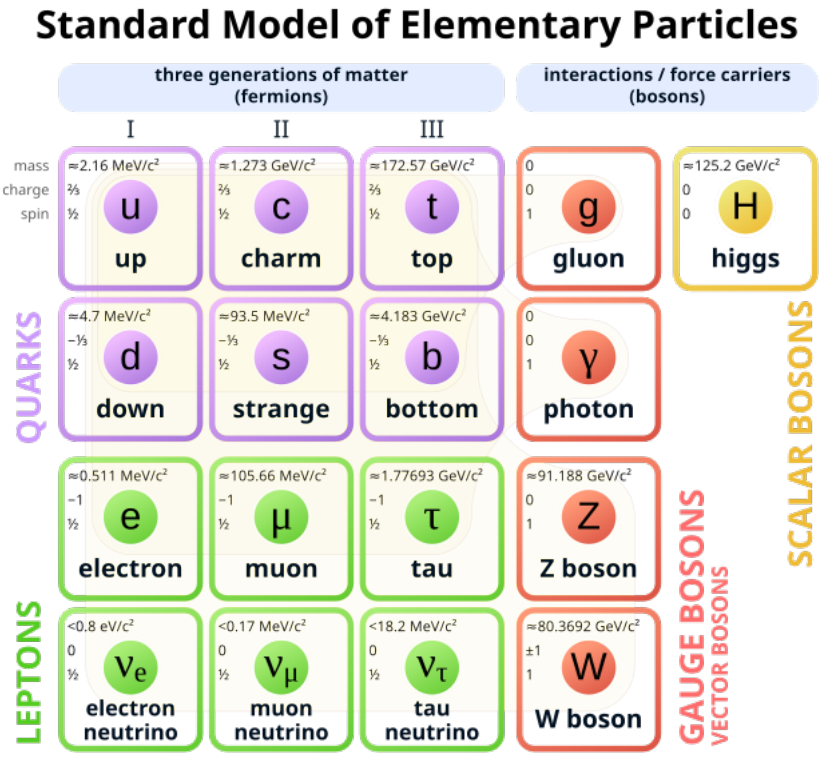

Figure 2.1: The standard model of particle physics, taken from [MC19].

The standard model consists of fermions (which have a half-integer spin) and bosons (which have an integer spin). The fermions have a spin of 1/2, whereas the bosons have a spin of 1, with exception of the Higgs-boson which has a spin of 0.

One class of fermions in the standard model consists of the six quarks, which make up hadrons. For example, a proton consists of two up quarks and one down quark and a neutron consists of two down quarks and one up quark. Quarks carry an electric charge and a colour charge, causing them to be subject to the electric and strong force respectively. The colour charge can be red, green or blue and their respective anti-colours. The total colour charge of a system needs to be white. One way to achieve this is by having a system consisting of a red, green and blue colour charge. Particles with this configuration (qqq) are called Baryons, like Protons and Neutrons. Another way of achieving a white colour charge is by putting together a quark and an antiquark ($q\bar{q}$). Such particles are called Mesons. The J/ψ Meson will be of high relevance later. More complex configurations are also possible. A single quark can not exist on its own. This is because quarks are subject to the strong force, and when two quarks are separated the energy being used to separate them will eventually be high enough to produce a new quark-antiquark pair. This property is referred to as confinement [Tho13].

The potential between two quarks caused by the strong force can be seen in Figure 2.2. The potential of the strong force has the form

$$V(r) = -\frac{4}{3}\frac{\alpha_s}{r} + \sigma r + constant \tag{2.1}$$

where r is the distance, α_s is the QCD running coupling constant and σ is the QCD string tension with 0.18 GeV^2 [BV98].

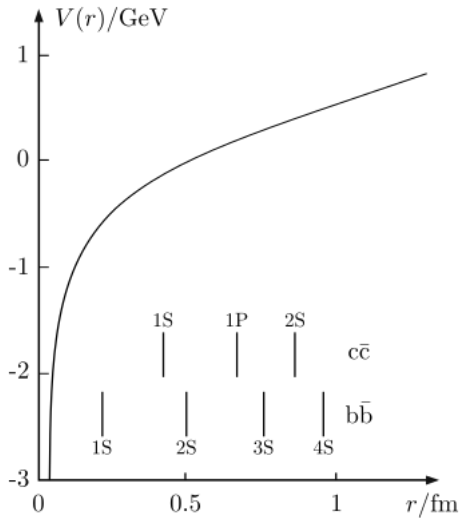

Figure 2.2: Potential between two quarks as a function of distance due to the strong interaction. Taken from [Com20].

The other class of Fermions are Leptons. Leptons are not subject to the strong interaction and can exist on their own. The most famous example is the electron. They do not carry a colour charge, but some of them can carry an electric charge, making them subject to the electromagnetic force.

Fermions make up matter, whereas vector bosons mediate forces. Gluons mediate the strong force, photons the electromagnetic force, whereas Z and W bosons mediate the weak force. As mentioned, the gravitational force can not be described by the standard model. Vector Bosons carry a spin, as opposed to scalar Bosons [Tho13].

2.1.1 The J/ψ meson

The J/ψ meson consists of a charm-anticharm quark pair. Particles made up of quark-antiquark pairs are referred to as quarkonia, making the J/ψ meson a Charmonium. The J/ψ meson is of special significance, since its discovery lead to the discovery of the charmonium quark [76a] [76b]. It has a rest mass of around 3097 MeV [Nak22].

When two protons collide with each other, J/ψ mesons can be produced promptly or non-promptly. The prompt processes are the decay of a heavier charmonium state

(e.g. ψ(2S)) into J/ψ or by hadronization due to a charm-anticharm pair not having enough energy to be separated and to produce another quark-antiquark pair, leading that pair to stay connected and to form a J/ψ meson [10]. The decay of a heavier charmonium state is a process often times described by non relativistic quantum chromodynamics (NRQCD) [BBL95]. The non-prompt production process happens via the decay of a beauty hadron (usually a B meson) [10].

2.2 Kinematic variables

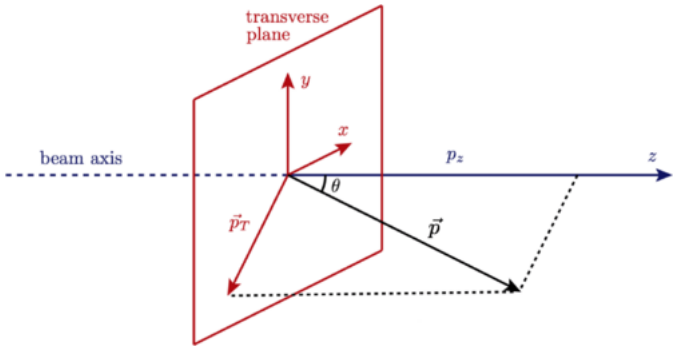

Figure 2.3: Geometry of a collider experiment. Taken from [Tan18].

In this section units are used such that $\hbar = c = 1$.

The four-momentum p is given by the Energy E and the three-momentum $\boldsymbol{p}$ of a particle as $p = (E, \boldsymbol{p})$.

In collider experiments the z-axis is usually defined along the beam direction. In this case p_z is the momentum along the beam axis, and p_T is defined as the momentum perpendicular to that and is also called the transverse momentum. The transverse momentum is then given by

$$p_T = \sqrt{(p_x^2 + p_y^2)}. \tag{2.2}$$

The polar angle is defined as

$$\theta = \arctan\left(\frac{p_T}{p_z}\right) \tag{2.3}$$

and can be seen in Fig. 2.3 [Fra23].

We can rescale the velocity and define

$$\beta_z = v_z/c \tag{2.4}$$

with v_z being the velocity along the z-axis and c the speed of light. The rapidity y is a quantity that maps β_z onto an interval of $(-\infty, \infty)$ and can be interpreted as generalized velocity [Rey17]. The energy and transverse momentum can also be used to define the rapidity [Fra23]

$$y = \frac{1}{2}\ln\left(\frac{1+\beta_z}{1-\beta_z}\right) = \frac{1}{2}\ln\left(\frac{E+p_z}{E-p_z}\right). \tag{2.5}$$

For $p \gg m$ the rapidity can be expanded

$$\begin{aligned} y &= \frac{1}{2}\ln\frac{\cos^2(\theta/2) + m^2/4p^2 + \dots}{\sin^2(\theta/2) + m^2/4p^2 + \dots} \\ &\approx -\ln\tan(\theta/2) \equiv \eta \end{aligned}$$

defining the pseudorapidity η [Tan18]. This is useful because η only depends on the polar angle θ, meaning that we can approximate the rapidity as pseudorapidity in particle collisions and detecting this angle is sufficient to determine it. This is because $p \gg m$ in particle collisions.

3 Experimental background

3.1 The Large Hadron Collider

The Large Hadron Collider is located in Switzerland and France and is the world's largest collider with a circumference of 26.7 km. The LHC is a synchrotron producing hadron beams. A sketch of it can be seen in Fig. 3.1.

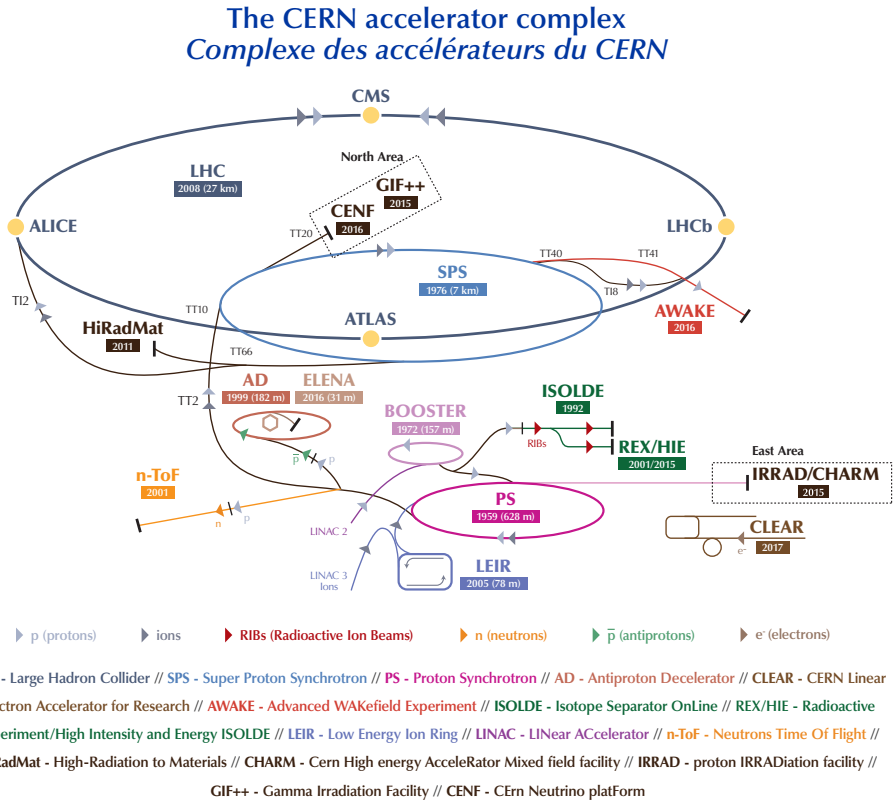

Figure 3.1: Sketch of the LHC. Taken from [Mob18].

The collider tunnel contains two beam pipes, which each accelerate one hadron beam. The two beam pipes are parallel to each other and the beams travel in opposite directions. Using dipole magnets the beam is kept on a circular path while the particles are being accelerated. The beam pipes meet at four different locations, leading to collision of the beams contained in these pipes. At one of these collision points the ALICE experiment is conducted, in which J/ψ particles are measured. The collision energy of a proton-proton collision is 13 TeV [EB08] and the Protons can be accelerated up to a speed of 0.999999990 c, with c being the speed of light [CER17].

3.2 ALICE

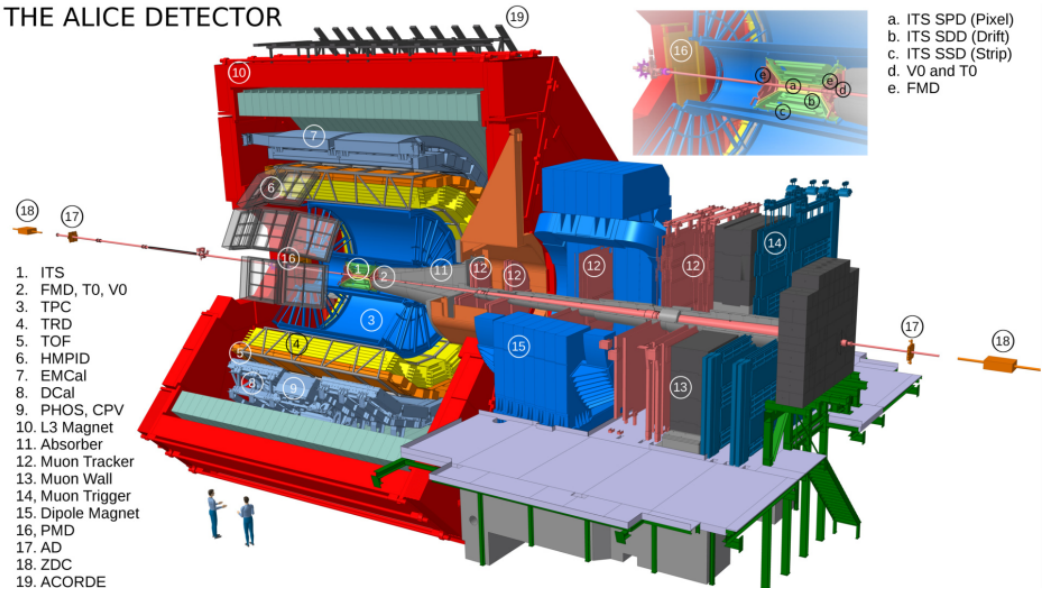

Figure 3.2: Schematic illustration of the ALICE detector. Taken from [Tau17].

The ALICE (A Large Ion Collider Experiment) detector is designed to study quark-gluon plasmas, which are created by lead-lead collisions [Col08]. It is thought that a quark-gluon plasma occured shortly after the Big-Bang [CER], which is why the ALICE experiment is used to investigate it. Additionally, the ALICE detector can also measure quarkonia created after pp-collisions.

The main part of the detector roughly has the shape of a cylinder with its central axis matching the beam axis containing the interaction point, and is called the central

barrel, as can be seen in Fig. 3.2. This central barrel consists of multiple layers made up of detectors. The innermost layer is the ITS. The ITS (Inner tracking system) is built around the beam pipe. The ITS in turn is surrounded by the TPC (Time-Projection Chamber). The outer edge of it has additional detectors installed on it.

3.2.1 The ITS, TPC and V0 detector

The ITS consists of multiple silicon layers, which cover the full azimuth angle but different pseudorapidity ranges. The Silicon Pixel Detector (SPD) consists of the two innermost layers, with which a pseudorapidity range of $|\eta| < 2$ and $|\eta| < 1.4$ can be measured respectively [Col08]. Using the SPD the charged particle multiplicity at mid-rapidity can be measured [Web18]. The third and fourth layer make up the Silicon Drift Detector (SDD) which cover a rapidity range of $|\eta| < 0.9$. The final two layers cover $|\eta| < 0.98$ and measure the energy loss $\frac{dE}{dx}$ of a particle, which can be used for particle identification. These layers form the Silicon Strip Detector (SSD).

The TPC is the primary detector used for particle identification and tracking charged particles. The TPC can has a pseudorapidity acceptance of $|\eta| < 0.9$. This allows charged particles from a J/ψ decay to be detected.

The V0 detector is a small angle detector. On both sides of the interaction point a scintillator array is located, referred to as V0A and V0C, which both make up the V0 detector. The V0A detector covers a pseudorapidity range of $2.8 < \eta < 5.1$, whereas the V0C detector covers a range of $-3.7 < \eta < -1.7$ [Col08].

4 PYTHIA event generator

4.1 PYTHIA

The simulations are conducted using the PYTHIA 8 event generator. PYTHIA 8 is a Monte Carlo event generator used for simulating high energy collisions, and in our case we will be studying pp collisions. Additionally $p\bar{p}$, e^+e^- and e^-e^- collisions can also be simulated. Every simulated event is provided with a list of all particles created during the collision. Also, information on a range of physical quantities are provided for each particle. A wide range of physical processes are implemented to describe the process, and they are explained in [SMS06] and [SMS08]. These physical processes can be taken into consideration with different parameters. These sets of parameters are also called tunes and in this case we are using the Monash 2013 tune, which is the most recent standard tune based on the state of research up until its implementation [SCR14].

4.2 Physics in PYTHIA

In the following the physics implemented in PYTHIA is described briefly.

The two hadrons (in our case protons) first exhibit initial state radiation before any collision takes place. One parton out of each beam starts branching into other partons, like e.g. $q \rightarrow qg$. The resulting partons can then do the same, resulting in an initial state shower. After that one or multiple partons out of the shower enter the hard process, i.e. collide. This produces outgoing partons and short lived resonances like for example $Z^0/W^{\pm}$. Similar to the the incoming partons, the outgoing partons can start branching out, resulting in final state radiation [SMS06].

Usually there are 4-10 Multiparton interactions (MPI) that take place at the LHC, which result in multiple perturbative scattering processes which are implemented in PYTHIA [SZ87]. That means that not only one parton out of the parton shower of each of the protons enters the hard interaction, but multiple. MPI can be turned on or off. Initial state radiation and final state radiation are also implemented.

There are also processes that do not involve this hard interaction that can take place. Due to the initial parton being taken out of the beam, the beam remnant can have a non-white color charge. The partons in the beam remnant can either form color singlet states or form strings. These strings can undergo string breaking as laid out before. That means, the partons are separated until they form quark-antiquark pairs. Thereby they can produce hadrons. This process is called hadronization. Creation of heavy quarks is negligible in this scenario, because their mass makes it unlikely to be produced via string breaking. Another type of hadronization is cluster collapse. Heavy quarks from parton showers and from the beam remnant connect via the strong force. If the potential energy is too low for string breaking, the heavy quarks collapse into a quarkonium. The created hadrons may be unstable and decay further [SMS06].

Hadronization is implemented via the Lund string fragmentation model. The partons after the collision are connected through strings carrying potential energy due to the strong force. As explained before, partons and gluons carry a colour charge, meaning if they are separated they stay connected through this string until the potential energy is high enough to produce another quark antiquark pair. This can happen multiple times until the individual strings do not carry enough energy to create another quark-antiquark pair and all the partons are bound to other partons. Cluster collapse is implemented too.

There is a property called Colour Reconnection (CR) which is also implemented in PYTHIA and can be turned on or off. This allows partons that are connected to different strings to swap their position and change the partons they are connected to [SMS06]. That process can already lower the potential energy stored in a string before the constituents of a string separate far enough to create quark-antiquark pairs. That can be seen as reducing the total string length. Since most particles are produced from the mechanism of separating partons creating quark-antiquark pairs, Colour Reconnection reduces the amount of created particles [AS14].

There are three ways in which J/ψ mesons can be produced. The first one is in the hard scattering process via NRQCD (non-relativistic quantum chromodynamics) mechanisms. This can be a gluon splitting into a heavy quark pair, or due to interactions of companion quarks in the process. Another contribution to the NRQCD mechanism is due to pQCD (perturbative quantum chromodynamics) mechanisms implemented in a pQCD matrix. These mechanisms are gluon fusion and light quark-antiquark annihilation. The second one is cluster collapse, as explained before. The third way of J/ψ being produced is via the decay of a beauty hadron (which in 95% of all cases is a B meson) [SMS06].

NRQCD mechanisms and cluster collapse are categorized as prompt production processes, whereas the decay of a beauty hadron is categorized as a non-prompt production process.

5 Previous studies

This chapter summarizes the results of a previous study, investigating the stronger than linear increase of self normalized mid-rapidity J/ψ yield with self normalized charged particle multiplicity using PYTHIA 8 [Web19]. In this summary we will mainly focus on the part of the study regarding the autocorrelation effects.

5.1 Simulation setup

A center of mass energy of 13 TeV was investigated for proton-proton collisions. The J/ψ meson is at mid-rapidity, meaning the rapidity of the investigated J/ψ mesons is $|y| < 0.8$. The investigated charged particles are either at mid-rapidity, which in this case is defined as the rapidity $|\eta| < 1$, or at forward (also called V0M) rapidity, defined as $2.8 < \eta < 5.1$ or $-3.7 < \eta < -1.7$. The default Monash 2013 tune was used. Also, different regions were investigated. The regions are defined using the angle $\Delta\phi$ with respect to the flight direction of the J/ψ:

$$\begin{aligned} \text{Toward region} &: \Delta\phi < \pi/3 \\ \text{Transverse region} &: \pi/3 < \Delta\phi < 2\pi/3 \\ \text{Away region} &: 2\pi/3 < \Delta\phi. \end{aligned}$$

The different regions are also illustrated in Fig. 5.1.

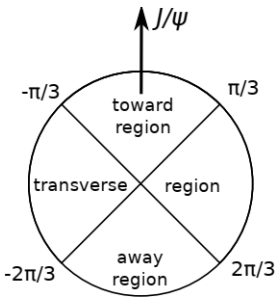

Figure 5.1: Definition of the different regions with respect to the J/ψ flight direction. Taken from [Web19].

5.2 Physics of the autocorrelation effects

The autocorrelation effects are described by multiple mechanisms. First, some of the J/ψ decay daughters are charged particles, contributing to the charged particle multiplicity. So if the multiplicity is measured in the same rapidity range as the J/ψ, which in our case is mid-rapidity, two additional charged particles are counted. Additionally, in NRQCD processes the J/ψ is produced together with a gluon which hadronizes and increases the charged particle multiplicity. If the state before the J/ψ state is a colour octet, an additional gluon is emitted during the transition to the J/ψ state. This happens under a small opening angle, hence most likely in the toward region. These autocorrelation effects for NRQCD processes and cluster collapse make up the autocorrelation effects of prompt production processes. For non-prompt production, the beauty hadron that decays into J/ψ has other decay daughters which can decay further. Also, the beauty quark that hadronized into the beauty hadron could have been accompanied by final state radiation, increasing the multiplicity in the surrounding region. Added to that, a high p_T parton is usually emitted in the direction opposite to the flight direction of the J/ψ particle, which lies in the away region. This parton fragments into a jet of particles. However, this may happen at a different rapidity than the rapidity of the J/ψ meson.

5.3 Results of the previous study

5.3.1 Results at mid- and forward rapidity

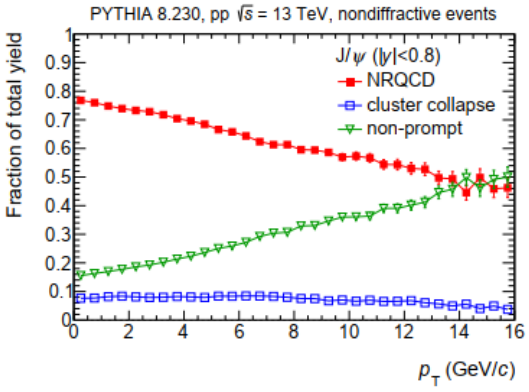

Figure 5.2: Relative contributions of different production processes to mid-rapidity J/ψ production as a function of transverse momentum p_T. Taken from [Web19].

In Fig. 5.2 it can be noted that the majority of the prompt particle production is carried out by NRQCD processes, whereas cluster collapse does not have a strong contribution to it (less than 20% of prompt particle production at most).

For mid-rapidity J/ψ production as a function of charged particle multiplicity, following behaviour was observed.

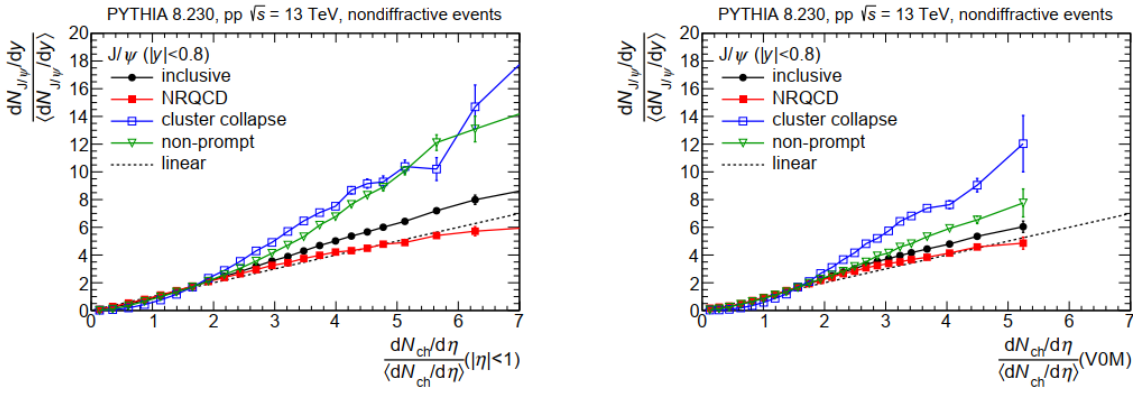

Figure 5.3: Mid-rapidity J/ψ production as a function of charged-particle multiplicity at mid (left) and forward (right) rapidity split into different production processes. MPI is turned on. Taken from [Web19].

In Figure 5.3 the self normalized mid-rapidity J/ψ yield from NRQCD grows linearly with the self-normalized charged particle multiplicity at both mid- and forward rapidity. The yield from cluster collapse grows stronger than linearly for both rapidity ranges. Non-prompt production grows stronger than linearly in both cases, however it grows stronger at mid-rapidity. This suggests autocorrelation effects for non-prompt J/ψ production. The linear yet strong growth that can be seen for NRQCD also hints to the possibility of some autocorrelation effects for prompt production. In Fig. 5.4 there is a high p_T dependence visible for both rapidity ranges, though it is stronger at mid-rapidity. This is mostly due to non-prompt J/ψ production.

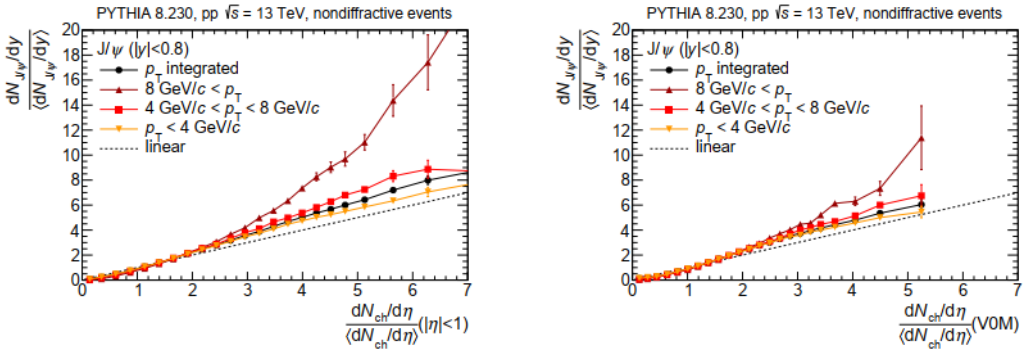

Figure 5.4: Mid-rapidity J/ψ production as a function of charged-particle multiplicity at mid (left) and forward (right) rapidity in different p_T intervals. MPI is turned on. Taken from [Web19].

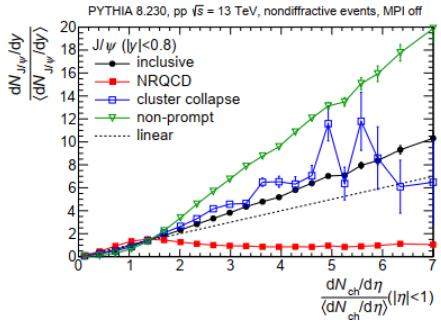

Figure 5.5: Mid-rapidity J/ψ production as a function of charged-particle multiplicity at mid-rapidity split into different production processes. MPI is turned off. Taken from [Web19].

For the now summarized investigation MPI was initially turned off to ensure that the J/ψ and charged particle production originate from the same process and what is

observed is indeed due to autocorrelation behaviour. However, even for MPI turned on similar autocorrelation patterns are expected.

The overall inclusive yield rises stronger than linearly with the self-normalized charged particle multiplicity, as can be seen in Fig. 5.5. It was observed that non-prompt J/ψ production increased very strongly with the number of charged particles. Similar for cluster collapse, but weaker. However, for J/ψ from NRQCD the self normalized yield increases with multiplicity until around 1.5 and then decreases. The explanation for this is following. Along with J/ψ, gluons are produced alongside. This initially leads to an increase because the gluons also contribute to J/ψ particle production. At higher multiplicites, there is competition between the charged particles and J/ψ, because the phase space is limited. This leads to a decrease of J/ψ if more charged particles take up the phase space. After these initial observations, the J/ψ production was again investigated as a function of the self normalized charged particle multiplicity, but this time for different regions and for the charged particle multiplicity at different rapidities.

5.3.2 Results for different regions

MPI was still turned off for this analysis. In this case mid- and forward rapidity were studied, as can be seen in Fig. 5.6.

NRQCD processes leading to J/ψ production are not strongly dependent on the charged particle multiplicity. Most charged particles during from this process are created in the flight direction of the J/ψ and less are created in other regions. That leads to a weak dependence of J/ψ yield on charged particle multiplicity in the toward region, an even weaker dependence in the transverse region, and almost no dependence in the away region. The non-prompt J/ψ yield at mid-rapidity is strongly dependent on the multiplicity in the away region and toward region, but less strongly dependent on multiplicity in the transverse region. J/ψ from cluster collapse at mid-rapidity is moderately dependent on the multiplicity in the away region and toward region and weakly dependent on the multiplicity in the transverse region at mid-rapidity.

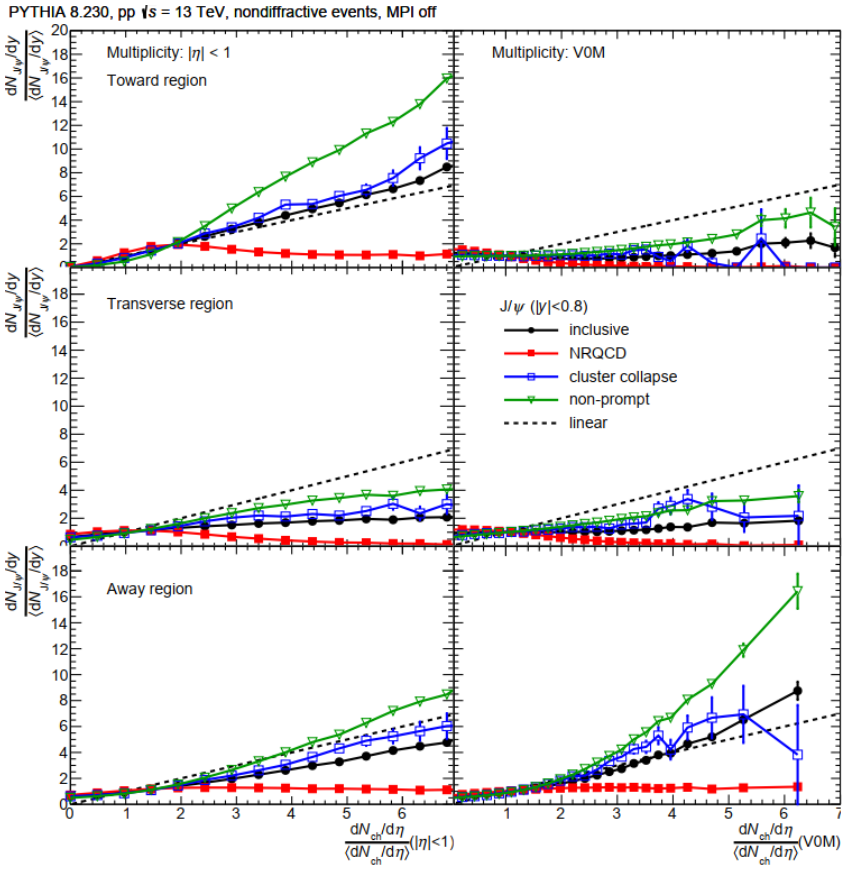

Figure 5.6: Mid-rapidity J/ψ production as a function of charged-particle multiplicity. Each panel shows the different production processes. The left side shows the multiplicity at mid rapidity, the right side shows the multiplicity at forward rapidity. The top row shows the toward region, the middle row the transverse region, and the bottom row the away region. MPI is turned off. Taken from [Web19].

The observations match the expectation from the effects contributing to autocorrelation earlier. The charged particle multiplicity in the region around the J/ψ is increased due to additional decay daughters, which in turn leads to another increase of the J/ψ production. The recoil jet also increases the multiplicity in the away region for a wide rapidity range, which is visible for non-prompt J/ψ.

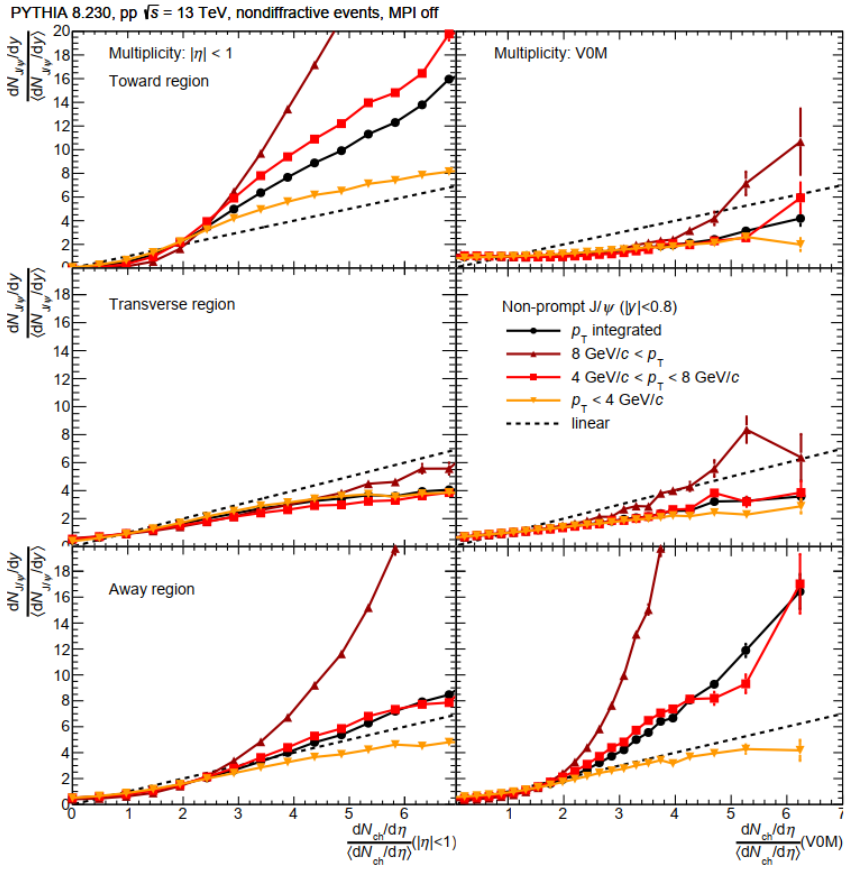

Figure 5.7: Mid-rapidity J/ψ production as a function of charged-particle multiplicity split in different p_T intervals. The left side shows the multiplicity at mid-rapidity, the right side shows the multiplicity at forward rapidity. The top row shows the toward region, the middle row the transverse region, and the bottom row the away region. MPI is turned off. Taken from [Web19].

Different transverse momentum p_T intervals were investigated, as can be seen in Figure 5.7. If autocorrelation effects are responsible for the stronger than linear increase for certain regions and rapidities, a stronger p_T dependence is expected for those. The reason for that also is that high p_T beauty quarks decay into more particles. As expected, the yield in the transverse region as a function of multiplicity at mid- and forward rapidity is mostly independent of p_T. Also, as expected, the J/ψ yield as a function of charged particle multiplicity in the toward region at forward rapidity is independent of changes in p_T. In principle non-prompt J/ψ production should not depend on the multiplicity in the transverse region. There is however a slight increase visible. This can be explained by analyzing the different production

mechanisms of the beauty quark, but will not be further discussed in this summary. It was discussed in the article ([Web19]).

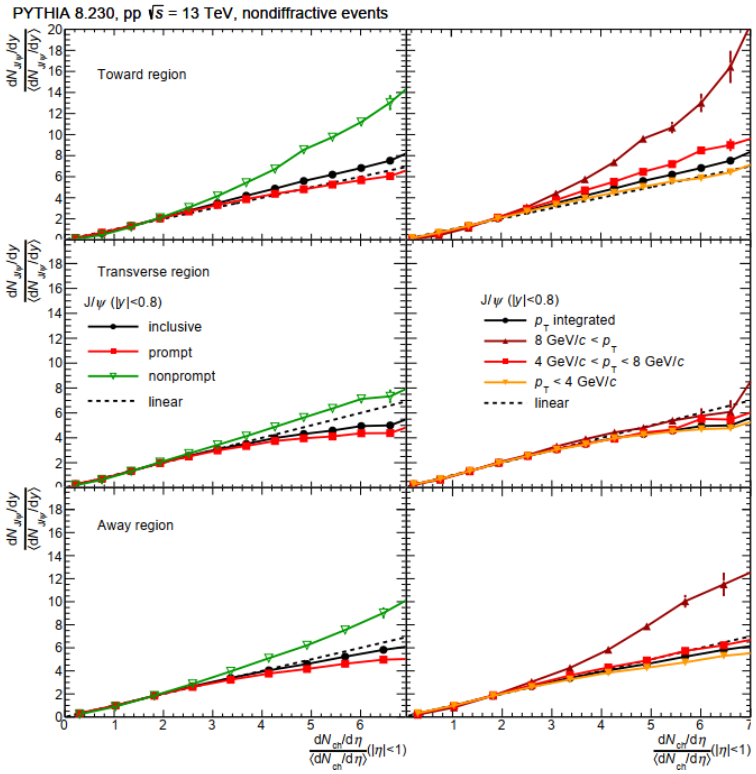

Figure 5.8: Mid-rapidity J/ψ production as a function of mid-rapidity charged-particle multiplicity. The left side shows the different production processes, the right side shows different p_T intervals. The top row shows the toward region, the middle row the transverse region, and the bottom row the away region. MPI is turned on. Taken from [Web19].

The previously explained investigations took place without considering MPI. However, the case with MPI was also reported and overall yielded similar results for the autocorrelation patterns, as can be seen in Figure 5.8. As before in the observations without MPI, non-prompt J/ψ yield grows stronger than linearly in the away and toward region. And as expected these regions also exhibit a higher dependency on p_T. The inclusion of MPI leads to an increase of the prompt J/ψ yield as a function of self normalized charged particle multiplicity. This was discussed in the article and will not be further discussed in this summary.

5.3.3 Charged hadron production

Mid-rapidity charged hadron production was also studied studied with different p_T intervals at mid-rapidity, as can be seen in Fig. 5.9. Similarly to J/ψ, a stronger than linear increase is visible and the nonlinearity is more pronounced at higher p_T as a function of charged particle multiplicity in the toward region. And similarly as for J/ψ, the different p_T intervals do not have an impact on the charged hadron production as a function of charged particle multiplicity in the transverse region. Still, autocorrelations have a small effect leading to a small deviation from the baseline (the linear function shown in Fig. 5.9). The meaning of the baseline was discussed in the article and will not be explained here.

This investigation served as a confirmation of the conclusion that the stronger than linear increase of J/ψ production and its p_T dependence is fully explained by autocorrelation effects.

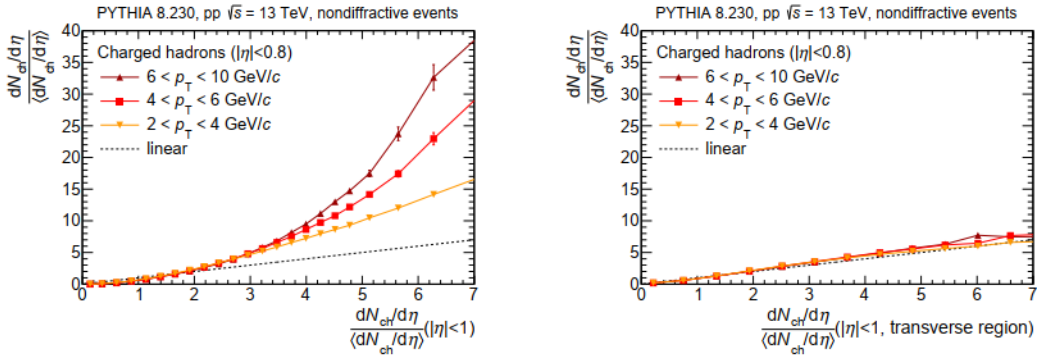

Figure 5.9: Mid-rapidity charged hadron production as a function of charged-particle multiplicity. Each panel shows the different p_T intervals. The left side shows the multiplicity at mid-rapidity, the right side shows the multiplicity at forward rapidity. MPI is turned on. Taken from [Web19].

6 Analysis and results

6.1 Simulation setup

In our analysis MPI (Multipartion interactions) were also considered and CR (Colour reconnection) was allowed. Even though MPI are allowed, autocorrelation effects should still be visible as mentioned before. We again investigate the mid-rapidity J/ψ production in pp collisions, more specifically, the self normalized mid-rapidity J/ψ yield $\frac{dN_{J/\psi}/dy}{\langle dN_{J/\psi}/dy\rangle}$ as a function of the self normalized charged particle multiplicity $\frac{dN_{ch}/d\eta}{\langle dN_{ch}/d\eta\rangle}$. We distinguished between prompt and non-prompt production, with cluster collapse and NRQCD processes considered prompt, and the decay of a beauty hadron considered non-prompt. The center of mass energy was 13 TeV. Charged particle multiplicity is defined according to the ALICE definition [17]. The definition of the different regions is the same as in the previous study, however in the following investigation $|y| < 0.9$ is defined as mid-rapidity for the J/ψ Meson. The investigated charged particle rapidity ranges were changed, to investigate the autocorrelation effects for different charged particle rapidities. As before, the default Monash 2013 tune was used. The considered events were nondiffractive, as in the previous study.

6.2 Results for different rapidities

6.2.1 Self normalized J/ψ production a function of the self normalized charged particle multiplicity in different rapidity ranges

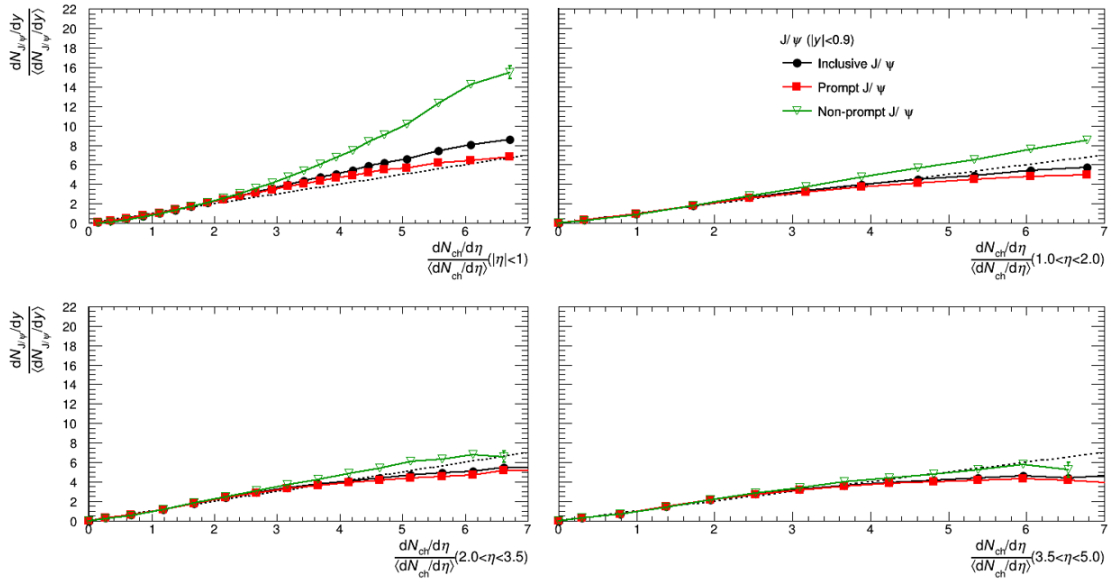

Figure 6.1: Self normalized mid-rapidity J/ψ production is shown as a function of the self normalized charged particle multiplicity in different rapidity ranges and split in different production processes.

In Fig. 6.1 the self normalized J/ψ production is shown as a function of the self normalized charged particle multiplicity in different rapidity ranges and for different production processes. For $|\eta| < 1$ the increase of the non-prompt self normalized J/ψ yield is stronger than linear, matching previous results. Prompt production processes grow roughly linearly, also matching previous results, considering that NRQCD processes contribute much more to non-prompt production than cluster collapse. The overall increase for that rapidity range is slightly stronger than linear for the charged particle multiplicity $\frac{dN_{ch}/d\eta}{\langle dN_{ch}/d\eta\rangle} < 5$ and roughly linear after that. For $1 < \eta < 2$ non-prompt J/ψ production grows linearly. Prompt production grows sligthly weaker than linearly. For $2 < \eta < 3.5$ non-prompt production grows roughly linearly and prompt production grows slightly weaker than linearly.

For $3.5 < \eta < 5$ non-prompt production also grows roughly linearly and prompt production grows weaker than linearly. However, for these rapidites the slope of the linear growth for non-prompt production processes is lower than for $1 < \eta < 2$ indicating lower autocorrelation effects. So for mid-rapidity J/ψ production previous results could be reproduced for $|\eta| < 1$. The other rapidities that have not been studied before show different behaviour, with non-prompt J/ψ increasing roughly linearly and prompt J/ψ increasing mostly weaker than linearly. The linear increase of non-prompt production indicates some autocorrelation effects that are not very strong, whereas the weaker than linear growth of prompt production indicates weak to no autocorrelation effects.

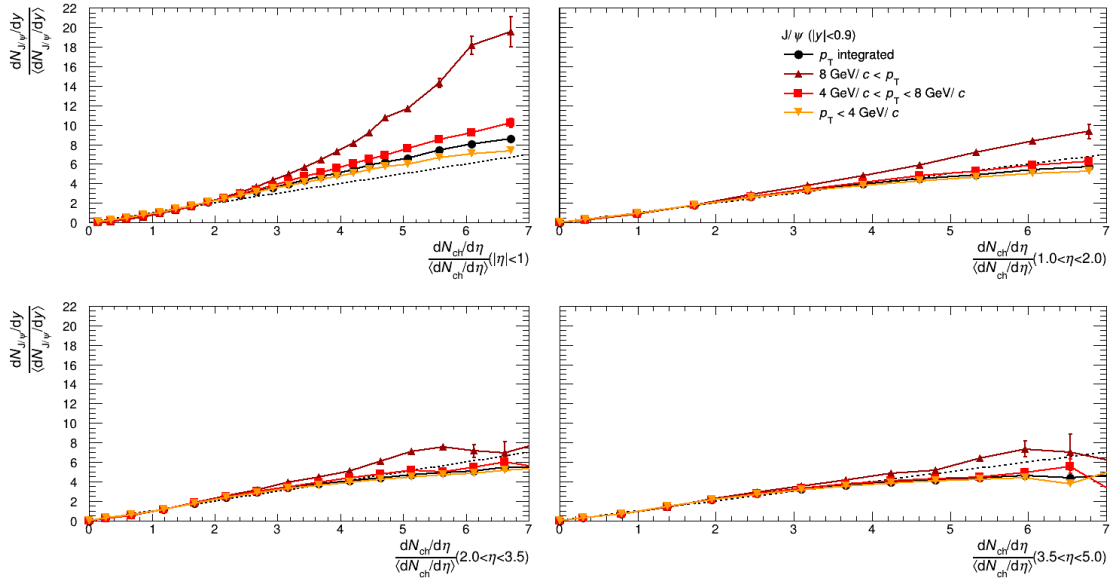

Figure 6.2: Self normalized mid-rapidity J/ψ production is shown as a function of the self normalized charged particle multiplicity in different rapidity ranges and split in different p_T intervals.

In Fig. 6.2 it is visible for $|\eta| < 1$ that there is a strong p_T dependence. The increase of self normalized mid-rapidity J/ψ production as a function of the self normalized charged particle multiplicity is much stronger than linear for $p_T > 8$ in this case. For the other p_T ranges a higher p_T leads to a moderately stronger increase. This is the same rapidity range in which the much stronger than linear increase for non-prompt J/ψ production was observed in Fig. 6.1. The same result was observed in the previous study. For $1 < \eta < 2$ a weaker dependence on p_T is observed. For

all p_T intervals the increase is linear. For $p_T > 8$ the slope of the linear increase is stronger than for the other p_T ranges. The other p_T ranges all grow with roughly the same slope. The weaker p_T dependence is in line with the observation that the increase of the self-normalized J/ψ yield at mid-rapidity as a function of self-normalized charged-particle multiplicity for this rapidity range is lower, as noted in Fig. 6.1. There is still a notable p_T dependence, which is in agreement with some weaker autocorrelation effects. For the remaining two rapidities the different p_T ranges exhibit a slightly weaker than linear increase of self-normalized J/ψ yield as a function of self-normalized charged particle yield. In these cases the slope of the growth at $p_T > 8$ is only slightly higher than for the other transverse momentum intervals, whereas the other p_T intervals roughly have the same slope. This matches the observations that these rapidity ranges did not show stronger than linear increase before and is in agreement with low to no autocorrelation effects.

6.2.2 Analysis of the production processes in different regions

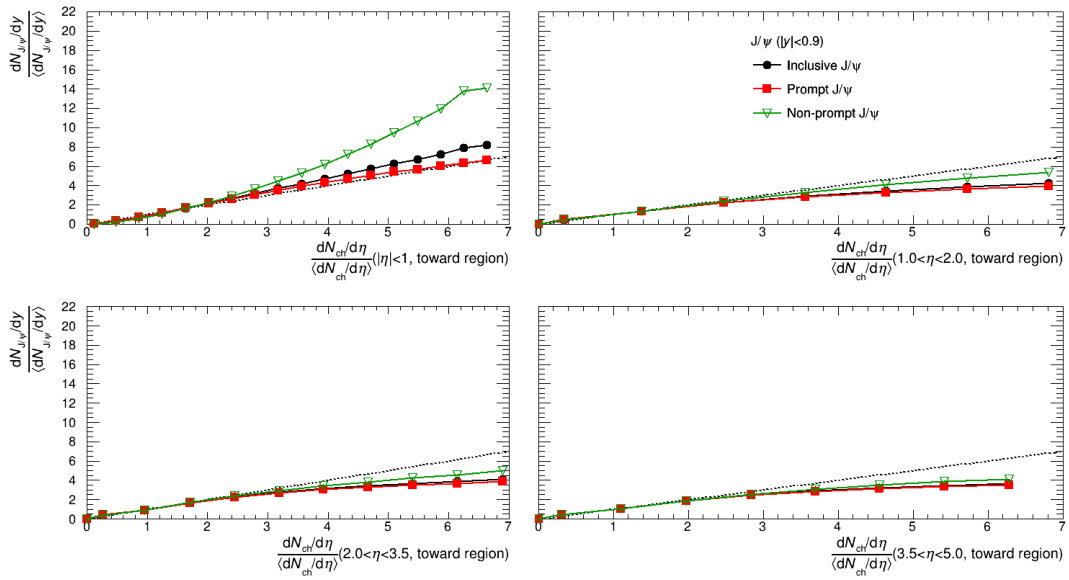

Figure 6.3: Self normalized mid-rapidity J/ψ production is shown as a function of the self normalized charged particle multiplicity in different rapidity ranges in the toward region and split in different production processes.

The results for the toward region can be seen in Figure 6.3. For $|\eta| < 1$ the overall stronger than linear increase is visible for the toward region and especially for the

non-prompt J/ψ production. For $1 < \eta < 2$ the increase is weaker than linear. For $2 < \eta < 3.5$ the behaviour is similar as for $1 < \eta < 2$, with weaker than linear growth for all production processes. For $3.5 < \eta < 5$ the increase is also weaker than linear for all production processes. The stronger than linear increase for $|\eta| < 1$ matches the observation the previous study of having strong autocorrelation effects for this rapidity in the toward region. However, the autocorrelation effects seem to be much lower for the other rapidities.

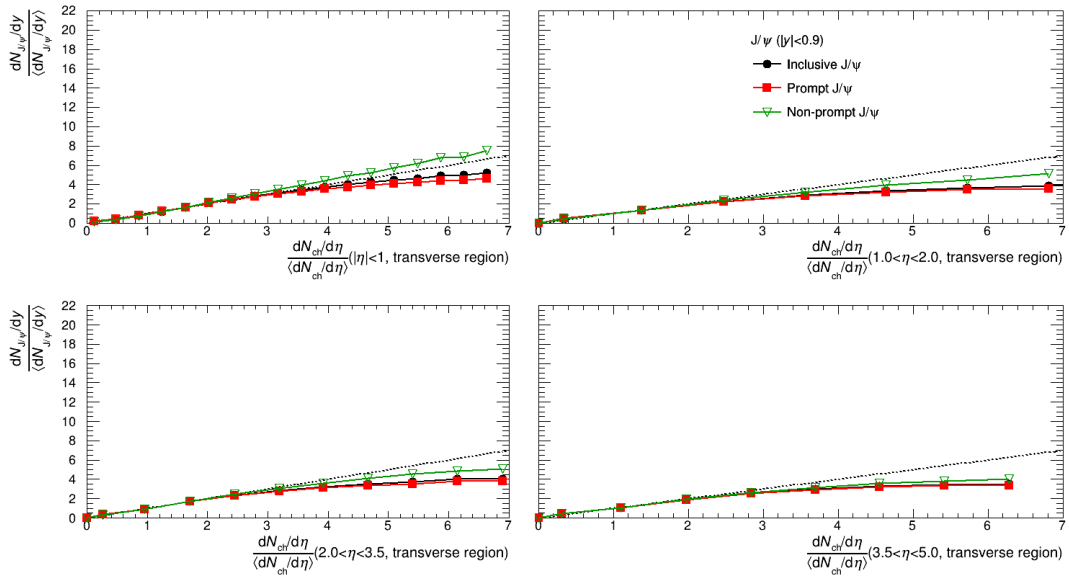

Figure 6.4: Self normalized mid-rapidity J/ψ production is shown as a function of the self normalized charged particle multiplicity in different rapidity ranges in the transverse region and split in different production processes.

The results for the transverse region can be seen in 6.4. For $|\eta| < 1$ In the transverse region the overall growth is weaker than linear, however non-prompt production grows roughly linearly. This is in line with the previous results showing that the autocorrelation effects are low in the transverse region. The reason for the linear growth of non-prompt production processes is likely due to the inclusion of MPI rather than autocorrelation effects, as it was the case in the previous study for the same rapidity range in the transverse region. In the case for $1 < \eta < 2$, the increase in the transverse region is weaker than linear and shows similar behaviour as the

forward region in this rapidity range. For $2 < \eta < 3.5$ the behaviour is again similar as the behaviour for $1 < \eta < 2$ in the forward and transverse region, i.e. all production processes contribute to a weaker than linear increase. For $3.5 < \eta < 5$ the production processes again yield a weaker than linear growth. So overall, as expected, the autocorrelation effects are very low in the transverse region.

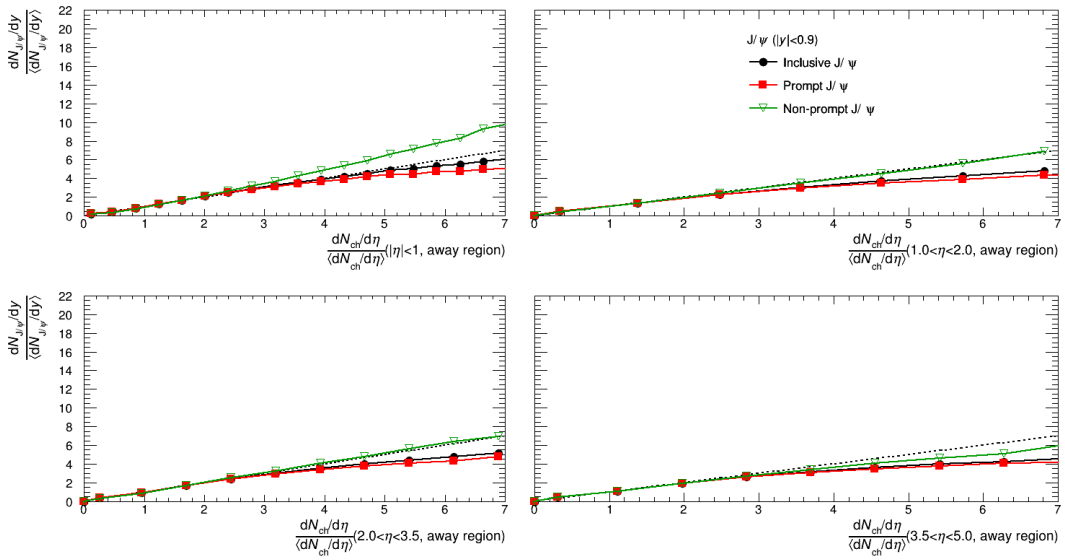

Figure 6.5: Self normalized mid-rapidity J/ψ production is shown as a function of the self normalized charged particle multiplicity in different rapidity ranges in the away region and split in different production processes.

The results for the away region can be seen in 6.5. In the away region a slightly stronger than linear increase can be observed for non-prompt J/ψ production, however the other production processes and the overall self normalized yield grow weaker than linear for $|\eta| < 1$, which indicates moderate autocorrelation effects. For $1 < \eta < 2$ the overall increase is weaker than linear, but non-prompt production shows a linear increase. For $2 < \eta < 3.5$ the same behaviour can be observed. This suggests some weak autocorrelation effects for non-prompt production and is in agreement with the fact that the recoil jet can be at a different rapidity than the initial b quark. For $3.5 < \eta < 5$ all production processes grow weaker than linear, indicating low or no autocorrelation effects in this region. However, the non-prompt production still grows stronger here than it does for the same rapidity in the toward and transverse region, albeit weaker than linearly. This could possibly be due to

some small influence of the recoil jet. So overall, the away region shows moderate autocorrelation effects, which are less pronounced than in the forward region, but stronger than in the transverse region. The appearance of some autocorrelation effects outside of mid-rapidity in the away region is in agreement with the fact that the recoil jet does not have to be at mid-rapidity, though it seems like the effect is still most pronounced at mid-rapidity.

6.2.3 Analysis of the transverse momentum dependence in different regions

It is expected that rapidities and regions that show autocorrelation effects exhibit a stronger p_T dependence.

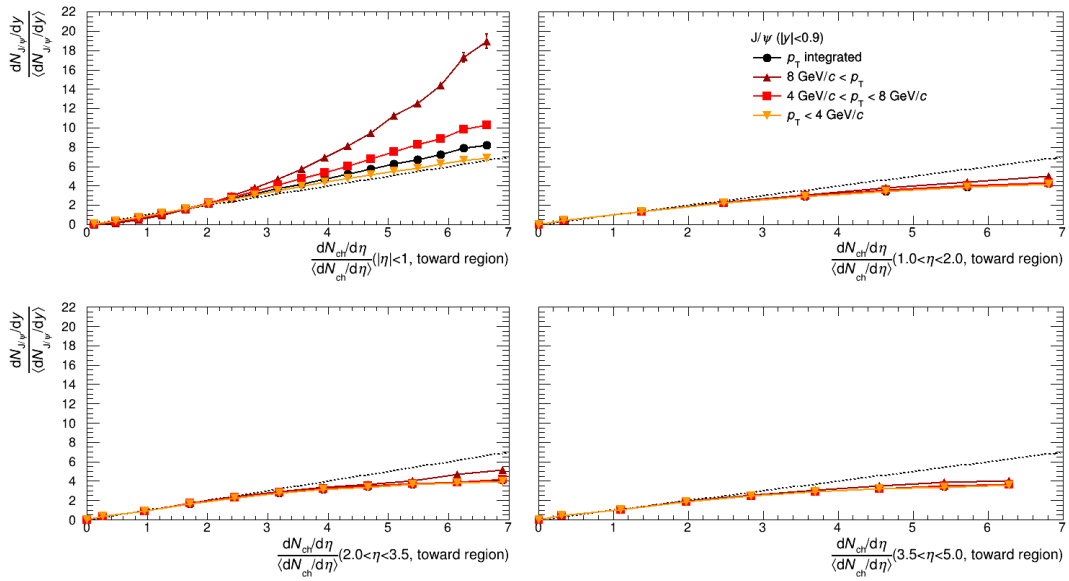

Figure 6.6: Self normalized mid-rapidity J/ψ production is shown as a function of the self normalized charged particle multiplicity in different rapidity ranges in the toward region and for different p_T intervals.

The results for the toward region can be seen in 6.6. For $|\eta| < 1$ in the toward region the increase for the inclusive J/ψ is stronger than linear, with $p_T > 8$ showing an especially strong nonlinear increase. In the plot for $1 < \eta < 2$ in Fig. 6.3 it was visible that the toward region did not exhibit strong autocorrelation behaviour for this rapidity. This is also visible here because the toward region has an increase

mostly independent of p_T with the increase being weaker than linear. The increase for $2 < \eta < 3.5$ is mostly p_T independent and weaker than linear. This is again in line with the fact that the previous plot for this rapidity range does not indicate strong autocorrelation effects. For $3.5 < \eta < 5$ the increase is independent of p_T here, which is again in line with the previous observation. For this region the p_T dependence observed in previous studies and expected due to the autocorrelation observed for $|\eta| < 1$ could be reproduced. The other regions show almost no p_T dependence, which is also in line with the lack of observed autocorrelation in the corresponding plots showing the different production processes.

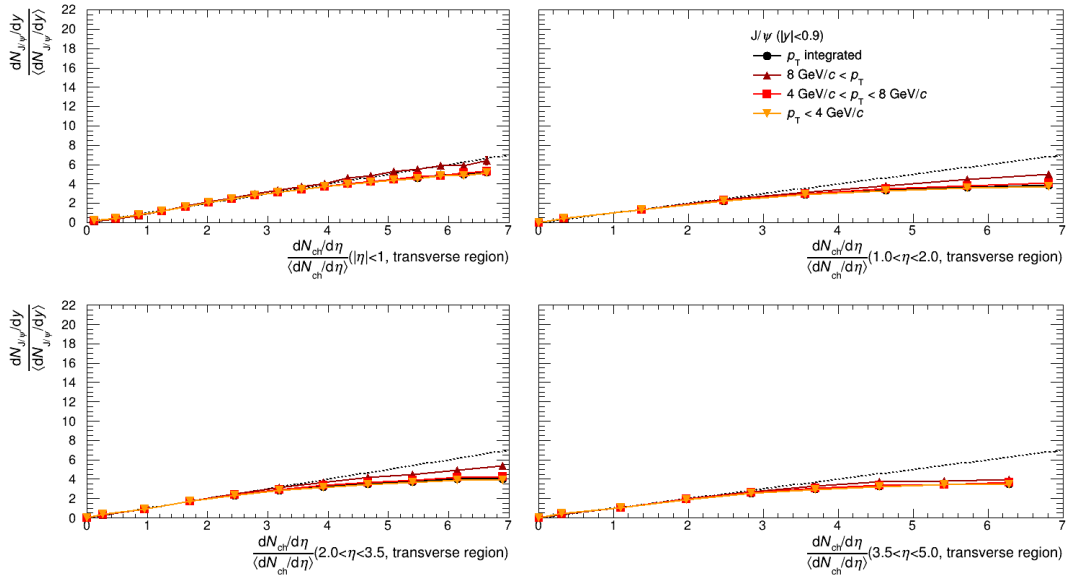

Figure 6.7: Self normalized mid-rapidity J/ψ production is shown as a function of the self normalized charged particle multiplicity in different rapidity ranges in the transverse region and for different p_T intervals.

The results for the transverse region can be seen in 6.7. As in the previous study, the transverse region does not show a strong p_T dependence for $|\eta| < 1$ and the overall increase is slightly weaker than linear. This is also in line with the fact that this region does not indicate strong autocorrelation effects in Fig. 6.4. For $1 < \eta < 2$ the overall increase is also weaker than linear and is mostly p_T independent. The same is the case for $2 < \eta < 3.5$ and $3.5 < \eta < 5$. So overall, the increase is mostly p_T independent, as expected for regions with low autocorrelation effects.

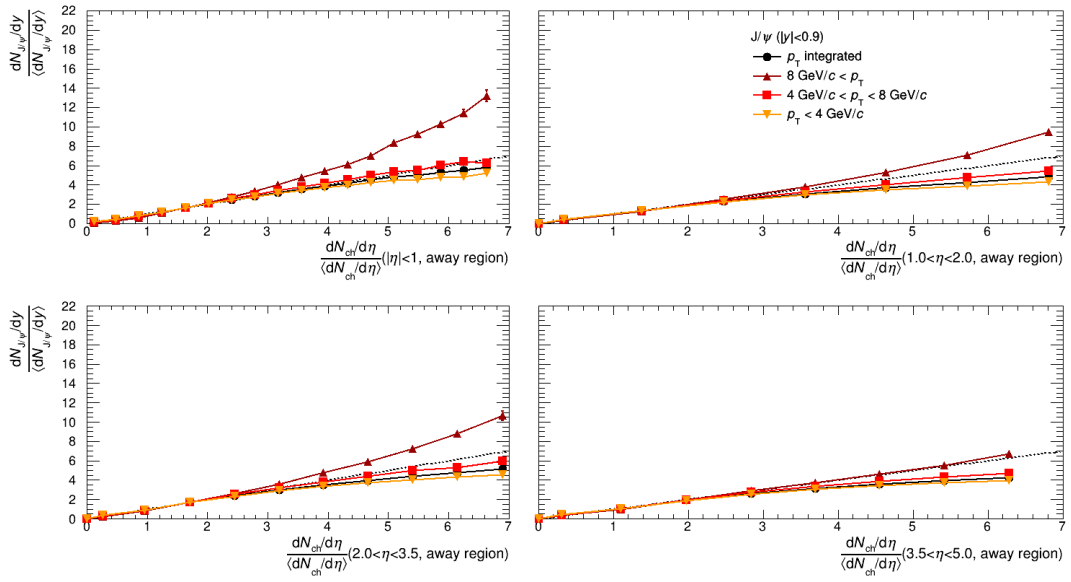

Figure 6.8: Self normalized mid-rapidity J/ψ production is shown as a function of the self normalized charged particle multiplicity in different rapidity ranges in the away region and for different p_T intervals.

The results for the away region can be seen in Fig. 6.8. For $|\eta| < 1$ in the away region the increase for the inclusive J/ψ is stronger than linear, with $p_T > 8$ showing an especially strong nonlinear increase. The increase is weaker in the away region than in the towards region (as can be seen in Fig. 6.6), which is also in line with the observation that the corresponding plot showcasing the production processes indicate moderate autocorrelation effects. For $1 < \eta < 2$ the overall increase in the away region is weaker than linear but has a moderate p_T dependence with $p_T > 8$ increasing stronger than linearly, which matches the slight autocorrelation behaviour observed before. For $2 < \eta < 3.5$ the away region showed similar slight autocorrelation effects, and accordingly a moderate p_T dependence can be observed for the away region, with $p_T > 8$ growing stronger than linearly. For $3.5 < \eta < 5$ the increase is linear for $p_T > 8$ in the away region. This is in line with the previous results also showing weaker than linear growth, but showing a slightly stronger growth (though still weaker than linear) for non-prompt production in the away region. This very weak p_T dependence is in agreement with very weak autocorrelation effects.

Overall it can be said that the autocorrelation effects are most strongly visible for $|\eta| < 1$ in the toward and away region and weaker autocorrelation effects are visible for the same regions at some other rapidities. $1 < \eta < 2$ and $2 < \eta < 3.5$ show some weak autocorrelation effects, and $3.5 < \eta < 5$ shows almost none or very weak autocorrelation effects for these regions. The transverse region is mostly unaffected by autocorrelation effects. In absence of autocorrelation effects a weaker than linear growth is noted. Non-prompt processes show much stronger autocorrelation effects and influences of the recoil jet can be noted in the away region.

6.2.4 Influence of different rapidities for each production process

To more clearly visualize the contributions of different rapidities, the different rapidities have been plotted for different regions for each production process.

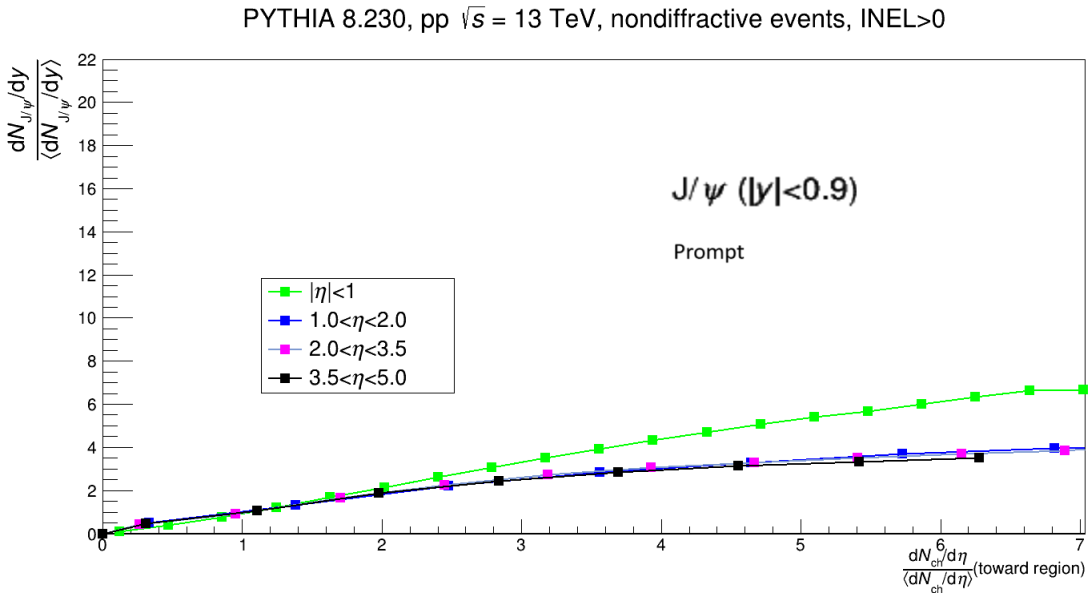

Figure 6.9: Prompt self normalized mid-rapidity J/ψ production is shown as a function of the self normalized charged particle multiplicity in the toward region and split in different rapidity ranges.

For prompt production in the toward region $|\eta| < 1$ shows the strongest growth. The increase is relatively strong, though not linear. The other rapidity ranges all show relatively weak growth (Figure 6.9).

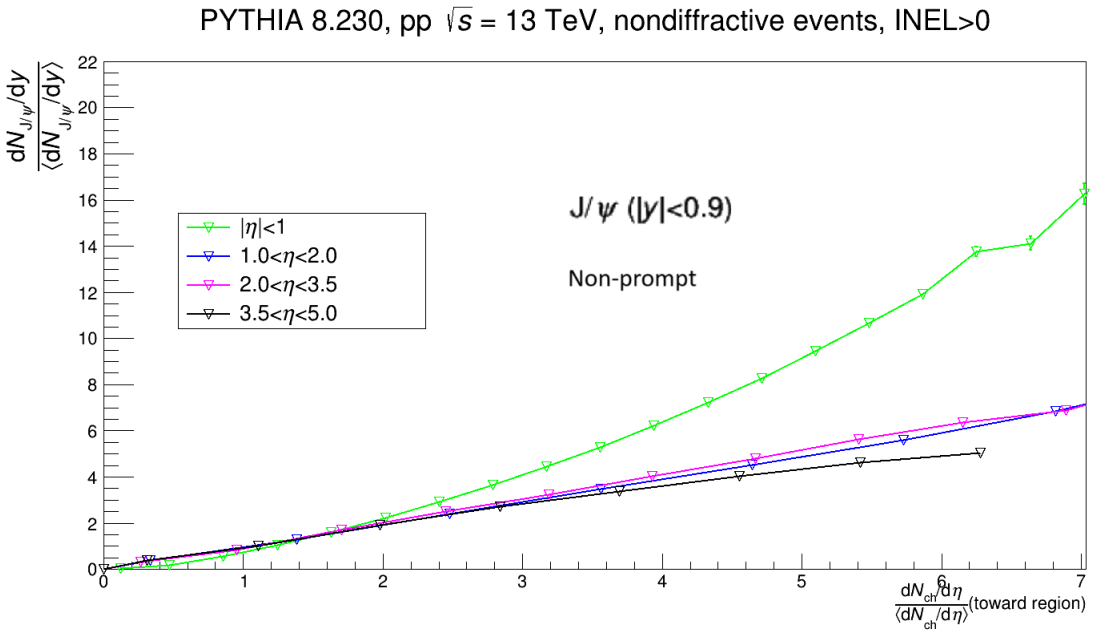

Figure 6.10: Non-prompt self normalized mid-rapidity J/ψ production is shown as a function of the self normalized charged particle multiplicity in the toward region and split in different rapidity ranges.

In Fig. 6.10 it can be seen that in the toward region there is a strong nonlinear increase for $|\eta| < 1$. For $1 < \eta < 2$ and $2 < \eta < 3.5$ the increase is roughly linear in the case of non-prompt production. For $3.5 < \eta < 5$ the increase is weaker than linear.

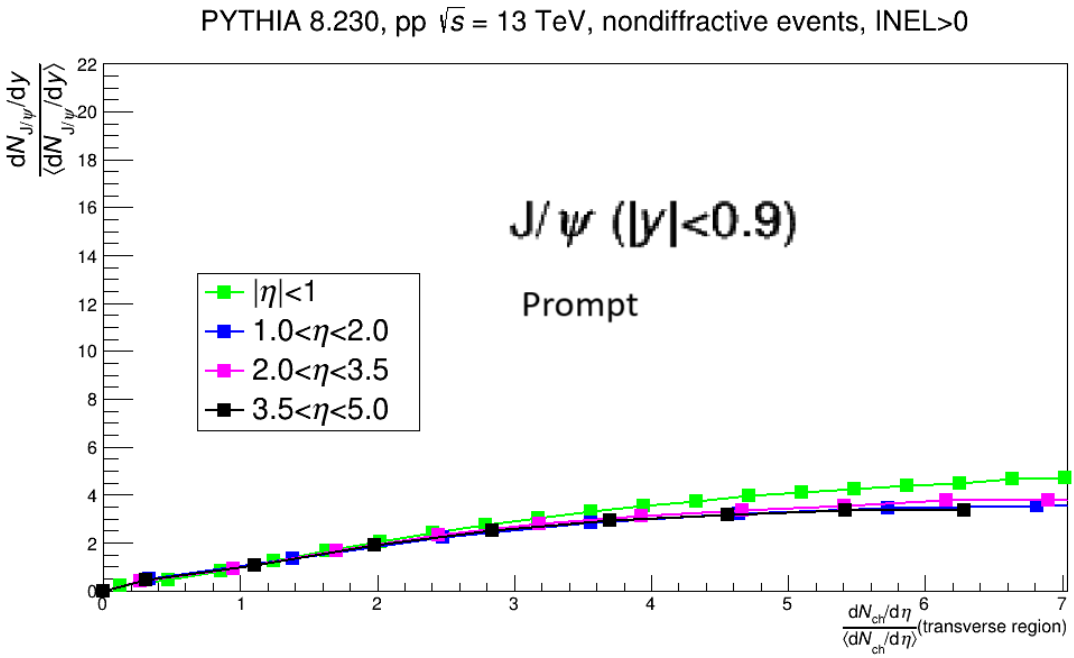

Figure 6.11: Prompt self normalized mid-rapidity J/ψ production is shown as a function of the self normalized charged particle multiplicity in the transverse region and split in different rapidity ranges.

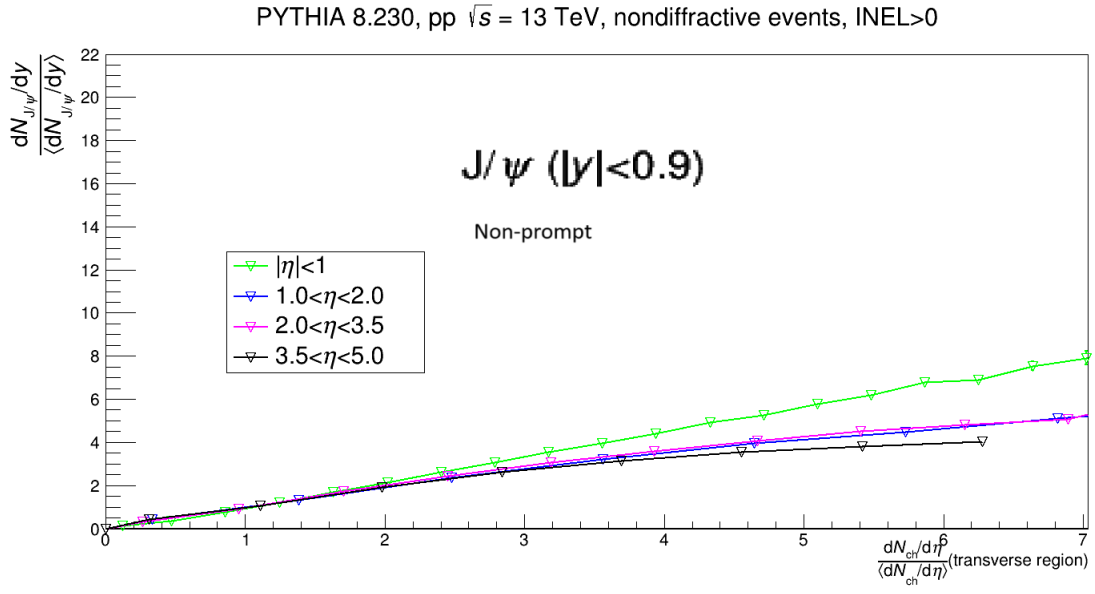

Figure 6.12: Non-prompt self normalized mid-rapidity J/ψ production is shown as a function of the self normalized charged particle multiplicity in the transverse region and split in different rapidity ranges.

As can be seen in Figure 6.11, the increase is weaker than linear in all cases, though $|\eta| < 1$ shows a slightly stronger increase than other rapidities for prompt production processes.

Looking at non-prompt production in the transverse region (6.12), $|\eta| < 1$ shows a moderately strong and linear growth, which is likely due to influence of multiparton interactions. $1 < \eta < 2$ and $2 < \eta < 3.5$ show a weak and lower than linear increase, which matches weak autocorrelation effects. $3.5 < \eta < 5$ shows a very low and much weaker than linear increase, which is in line with very low or almost no autocorrelation contribution.

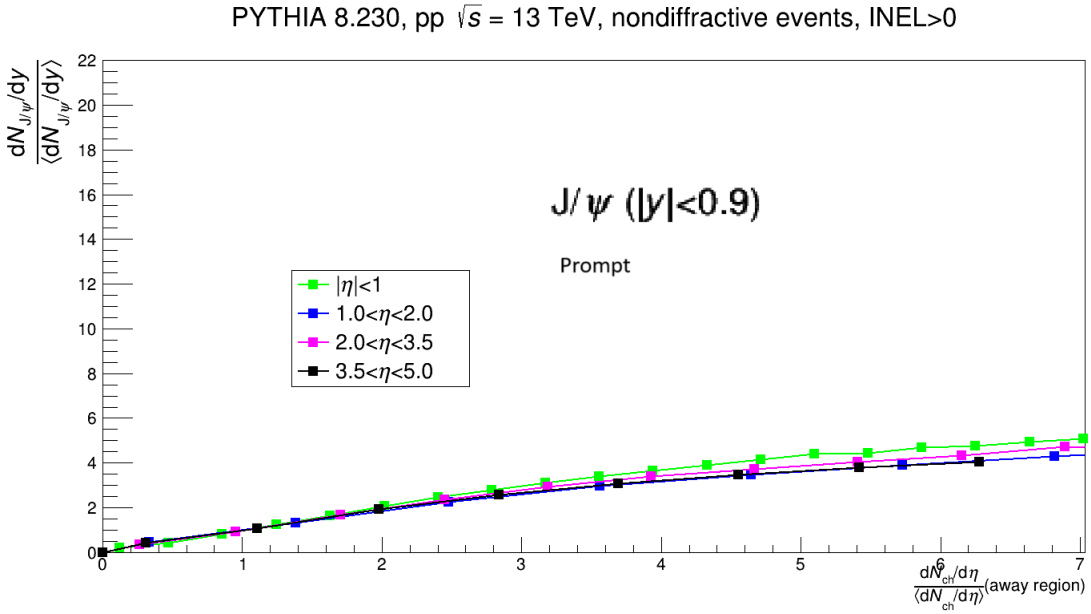

Figure 6.13: Prompt self normalized mid-rapidity J/ψ production is shown as a function of the self normalized charged particle multiplicity in the away region and split in different rapidity ranges.

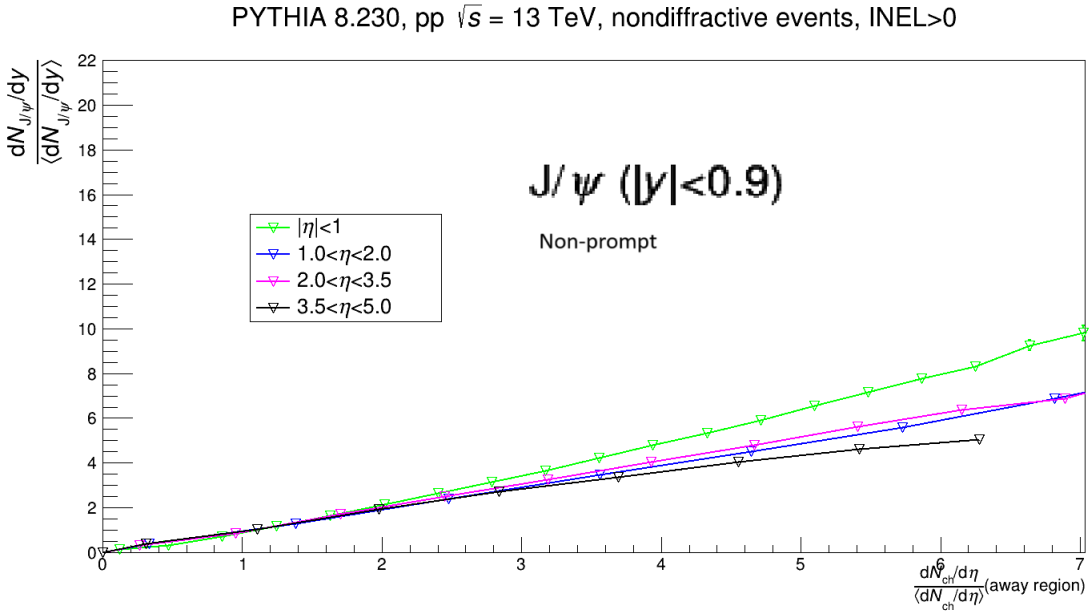

Figure 6.14: Non-prompt self normalized mid-rapidity J/ψ production is shown as a function of the self normalized charged particle multiplicity in the away region and split in different rapidity ranges.

All rapidities in the away region show roughly the same weaker than linear increase for prompt J/ψ production, as can be seen in Fig. 6.13.

For non-prompt processes in that region, as can be seen in Fig. 6.14, $|\eta| < 1$ shows a stronger than linear increase, which is in line with moderate autocorrelation effects. $1 < \eta < 2$ and $2 < \eta < 3.5$ grow linearly, which is in line with some weak autocorrelation effects. And $3.5 < \eta < 5$ grows slightly weaker than linearly, indicating very weak autocorrelation effects.

As an overall trend, the further away the rapidity is from mid-rapidity, the weaker the autocorrelation effects for mid-rapidity J/ψ production as a function of self normalized charged particle yield. Non-prompt processes exhibit stronger autocorrelation effects.

7 Conclusion and outlook

In this thesis the self normalized mid-rapidity J/ψ yield was investigated as a function of the self normalized charged particle multiplicity in different rapidity ranges. Different regions were also investigated. This was done by using data created in simulated pp collisions using PYTHIA 8, with a center of mass energy of 13 TeV. The resulting autocorrelation effects were analyzed and compared to previous results.

Initially the different production mechanisms of the J/ψ meson were analyzed. The overall increase of the self normalized J/ψ yield was stronger than linear with increasing charged particle multiplicity. This is mainly due to non-prompt production processes, and it mainly occurs in the forward and away region. These autocorrelation effects are primarily visible for charged particle rapidities with $|\eta| < 1$ and are less pronounced for other rapidity ranges, namely $1 < \eta < 2$, $2 < \eta < 3.5$ and $3.5 < \eta < 5$. $1 < \eta < 2$ and $2 < \eta < 3.5$ showed some weak to moderate autocorrelation effects whereas $3.5 < \eta < 5$ exhibited very weak to no autocorrelation effects. The stronger than linear increase was primarily present in the toward and away region. An influence of the recoil jet in non-prompt production could also be noted in the away region. The away and toward region are the regions in which autocorrelation effects were expected, as opposed to the transverse region where minimal autocorrelation effects were expected. The results for the regions matched the observations from a previous study [Web19]. These expectations could additionally be confirmed by looking at the self normalized J/ψ yield as a function of charged particle yield, but this time split into different transverse momentum p_T intervals. Rapidities in regions that showed stronger than linear growth showed a strong p_T dependence for the growth of the self normalized J/ψ yield. This again is in line with observations of the previous study, in which a stronger than linear increase was linked with a strong p_T dependence [Web19]. As before the transverse

region is largely p_T independent. Regions and rapidities not exhibiting this p_T dependence show a lower than linear increase. It can be concluded that autocorrelation behaviour is mostly responsible for a stronger than linear increase. Rapidities further away from mid-rapidity show less autocorrelation effects for mid-rapidity J/ψ production.

So overall, it can be confirmed that it is advisable to measure in the transverse region to minimize autocorrelation effects. Another way to reduce autocorrelation effects is to measure the rapidity range of $3.5 < \eta < 5$, however the ALICE detector is not capable of that, which is why this could be a future consideration.

Bibliography

[10] *J/Psi prompt and non-prompt cross sections in pp collisions at sqrt(s) = 7 TeV*. Tech. rep. Last accessed 18.03.2025. Geneva: CERN, 2010. URL: https://cds.cern.ch/record/1279616.

[17] "The ALICE definition of primary particles". In: (2017). URL: https://cds.cern.ch/record/2270008.

[76a] *Burton Richter*. Last accessed 15.03.2025. 1976. URL: https://www.nobelprize.org/prizes/physics/1976/richter/facts/.

[76b] *Samuel C.C. Ting*. Last accessed 15.03.2025. 1976. URL: https://www.nobelprize.org/prizes/physics/1976/richter/facts/.

[Abe12] B. Abelev et al. "J/ψ production as a function of charged particle multiplicity in pp collisions at √s = 7 TeV". In: *Physics Letters B* 712.3 (June 2012), pp. 165–175. ISSN: 0370-2693. DOI: 10.1016/j.physletb.2012.04.052. URL: http://dx.doi.org/10.1016/j.physletb.2012.04.052.

[AS14] Spyros Argyropoulos and Torbjörn Sjöstrand. "Effects of color reconnection on $t\bar{t}$ final states at the LHC". In: *Journal of High Energy Physics* 2014.11 (Nov. 2014). ISSN: 1029-8479. DOI: 10.1007/jhep11(2014)043. URL: http://dx.doi.org/10.1007/JHEP11(2014)043.

[BBL95] G. T. Bodwin, E. Braaten, and G. P. Lepage. "Rigorous QCD analysis of inclusive annihilation and production of heavy quarkonium". In: *Physical Review D* 51 (1995). [Erratum: Phys. Rev. D55, 5853 (1997)], pp. 1125–1171. eprint: hep-ph/9407339.

[BV98] Nora Brambillaa and Antonio Vairo. “Quark confinement and the hadron spectrum”. In: *Strong interactions at low and intermediate energies. Proceedings, 13th Annual Hampton University Graduate Studies, HUGS 98* (1998), pp. 151–220.

[CER] CERN. *ALICE Experiment*. Last accessed 18.03.2025. URL: https://home.cern/science/experiments/alice.

[CER17] CERN. *CERN Brochure 2017-002*. Last accessed 18.03.2025. 2017. URL: https://cds.cern.ch/record/2255762/files/CERN-Brochure-2017-002-Eng.pdf.

[Col08] The ALICE Collaboration et al. “The ALICE experiment at the CERN LHC”. In: *Journal of Instrumentation* 3 (Aug. 2008), S08002. DOI: 10.1088/1748-0221/3/08/S08002.

[Com20] Wikimedia Commons. *File:Strong Interaction Potential.svg — Wikimedia Commons, the free media repository*. Last accessed 16.03.2025. 2020. URL: https://commons.wikimedia.org/w/index.php?title=File:Strong_Interaction_Potential.svg&oldid=448045716.

[EB08] Lyndon Evans and Philip Bryant. “LHC Machine”. In: *Journal of Instrumentation* 3 (Aug. 2008), S08001. DOI: 10.1088/1748-0221/3/08/S08001.

[FP12] E. G. Ferreiro and C. Pajares. “High multiplicity pp events and J/ψ production at energies available at the CERN Large Hadron Collider”. In: *Physical Review C* 86.3 (Sept. 2012). ISSN: 1089-490X. DOI: 10.1103/physrevc.86.034903. URL: http://dx.doi.org/10.1103/PhysRevC.86.034903.

[Fra23] Roberto Franceschini et al. “Kinematic variables and feature engineering for particle phenomenology”. In: *Reviews of Modern Physics* 95.4 (Nov. 2023), p. 045004. DOI: 10.1103/RevModPhys.95.045004. URL: https://link.aps.org/doi/10.1103/RevModPhys.95.045004.

[MC19] MissMJ and Cush. *File:Standard Model of Elementary Particles.svg*. Last accessed 15.03.2025. 2019. URL: https://en.wikipedia.org/wiki/File:Standard_Model_of_Elementary_Particles.svg.

[Mob18] Esma Mobs. *The CERN accelerator complex-August 2018*. Tech. rep. 2018.

[Nak22] K. Nakamura et al. "J/ψ(1S)". In: *Journal of Physics G* 37.7A (2022). PDF version available from the Particle Data Group website, p. 075021. DOI: 10.1088/0954-3899/37/7A/075021. URL: https://pdg.lbl.gov/2022/listings/contents_listings.html.

[Rey17] Klaus Reygers. *Quark Gluon Plasma Physics, 2. Kinematic variables*. 2017. URL: https://www.physi.uni-heidelberg.de/~reygers/lectures/2017/qgp/qgp_ss17_02_kinematics.pdf.

[SCR14] P. Skands, S. Carrazza, and J. Rojo. "Tuning PYTHIA 8.1: the Monash 2013 tune". In: *The European Physical Journal C* 74.8 (Aug. 2014). ISSN: 1434-6052. DOI: 10.1140/epjc/s10052-014-3024-y. URL: http://dx.doi.org/10.1140/epjc/s10052-014-3024-y.

[SMS06] Torbjörn Sjöstrand, Stephen Mrenna, and Peter Skands. "PYTHIA 6.4 physics and manual". In: *Journal of High Energy Physics* 2006.05 (May 2006), pp. 026–026. ISSN: 1029-8479. DOI: 10.1088/1126-6708/2006/05/026. URL: http://dx.doi.org/10.1088/1126-6708/2006/05/026.

[SMS08] Torbjörn Sjöstrand, Stephen Mrenna, and Peter Skands. "A brief introduction to PYTHIA 8.1". In: *Computer Physics Communications* 178.11 (June 2008), pp. 852–867. ISSN: 0010-4655. DOI: 10.1016/j.cpc.2008.01.036. URL: http://dx.doi.org/10.1016/j.cpc.2008.01.036.

[SZ87] Torbjorn Sjostrand and Maria van Zijl. "A Multiple Interaction Model for the Event Structure in Hadron Collisions". In: *Phys. Rev. D* 36 (1987), p. 2019. DOI: 10.1103/PhysRevD.36.2019.

[Tan18] M. Tanabashi et al. "Review of Particle Physics". In: *Physical Review D* 98 (2018). and 2019 update, p. 030001.

[Tau17] Arturo Tauro. "ALICE Schematics". General Photo. 2017. URL: https://cds.cern.ch/record/2263642.

[Tho13] Mark Thomson. *Modern Particle Physics*. Cambridge University Press, 2013. DOI: 10.1017/CBO9781139525367.

[Web18] Steffen Georg Weber. "Multiplicity dependent J/ψ production in proton-proton collisions at the LHC". en. PhD thesis. Darmstadt: Technische Universität Darmstadt, Aug. 2018. URL: http://tuprints.ulb.tu-darmstadt.de/8461/.

[Web19] S. G. Weber et al. “Elucidating the multiplicity dependence of J / ψ production in proton–proton collisions with PYTHIA8”. In: *The European Physical Journal C* 79.1 (Jan. 2019). ISSN: 1434-6052. DOI: 10.1140/epjc/s10052-018-6531-4. URL: http://dx.doi.org/10.1140/epjc/s10052-018-6531-4.